Dosimetric impact of respiratory motion, interfraction baseline shifts, and anatomical changes in radiotherapy of non-small cell lung cancer

Mai Lykkegaard Schmidt, Lone Hoffmann, Maria Kandi, Ditte S. Møller & Per Rugaard Poulsen

ORIGINAL ARTICLE

Dosimetric impact of respiratory motion, interfraction baseline shifts, and anatomical changes in radiotherapy of non-small cell lung cancer

MAI LYKKEGAARD SCHMIDT[1], LONE HOFFMANN[2], MARIA KANDI[1], DITTE S. MØLLER[2] & PER RUGAARD POULSEN[1,3]

[1]*Department of Oncology, Aarhus University Hospital, Aarhus, Denmark,* [2]*Department of Medical Physics, Aarhus University Hospital, Aarhus, Denmark, and* [3]*Institute of Clinical Medicine, Aarhus University, Aarhus, Denmark*

Abstract

Background. The survival rates for patients with non-small cell lung cancer (NSCLC) may be improved by dose escalation; however, margin reduction may be required in order to keep the toxicity at an acceptable level. In this study we have investigated the dosimetric impact of tumor motion and anatomical changes during intensity-modulated radiotherapy (IMRT) of patients with NSCLC. *Material and methods.* Sixteen NSCLC patients received IMRT with concomitant chemotherapy. The tumor and lymph node targets were delineated in the mid-ventilation phase of a planning 4DCT scan (CT1). Typically 66 Gy was delivered in 33 fractions using daily CBCT with bony anatomy match for patient setup. The daily baseline shifts of the mean tumor position relative to the spine were extracted from the CBCT scans. A second 4DCT scan (CT2) was acquired halfway through the treatment course and the respiratory tumor motion was extracted. The plan was recalculated on CT2 with and without inclusion of the respiratory tumor motion and baseline shifts in order to investigate the impact of tumor motion and anatomical changes on the tumor dose. *Results.* Respiratory tumor motion was largest in the cranio-caudal (CC) direction (range 0–13.1 mm). Tumor baseline shifts up to 18 mm (CC direction) and 24 mm (left-right and anterior-posterior) were observed. The average absolute difference in CTV mean dose to the primary tumor (CTV-t) between CT1 and CT2 was 1.28% (range 0.1–4.0%) without motion. Respiratory motion and baseline shifts lead to average absolute CTV-t mean dose changes of 0.46% (0–1.9%) and 0.65% (0.0–2.1%), respectively. For most patients, the changes in the CTV-t dose were caused by anatomical changes rather than internal target motion. *Conclusion.* Anatomical changes had larger impact on the target dose distribution than internal target motion. Adaptive radiotherapy could be used to achieve better target coverage throughout the treatment course.

Local failure rates in radiotherapy of non-small cell lung cancer (NSCLC) are high and contribute to a low overall survival [1]. For this patient group improvements in radiotherapy (RT) should therefore aim at increased local control rates by assuring that the target receives the planned dose, or preferably an escalated dose, without compromising the organs at risk [2,3]. Intensity-modulated RT (IMRT) have proved useful for delivering target doses with high degree of conformity in NSCLC [4]. Dose conformation requires accurate knowledge of the patient and target geometry, but this is complicated by anatomical changes and internal tumor motion throughout the treatment course. Anatomical changes include tumor shrinkage [5–7] and lung density changes,

while the internal tumor motion include interfraction baseline shifts of the mean tumor position [8–10] and intrafraction motion due to, i.e. respiration and cardiac motion [11–13]. All these changes introduce uncertainty in the IMRT delivery and may compromise the optimal target coverage. While previous studies have examined the intra- and interfractional tumor motion few studies has investigated the dosimetric effects of intra- and interfractional tumor motion contrasted against anatomical changes during the treatment course. In the present retrospective study, we investigated how the intrafractional respiratory motion, the interfractional baseline shifts, and the anatomical changes impacted the delivered dose distribution to the primary tumor for a group of NSCLC patients.

Correspondence: M. L. Schmidt, Department of Oncology, Aarhus University Hospital, Noerrebrogade 44, Building 5, 2nd Floor, 8000 Aarhus C, Denmark. E-mail: maiscmid@rm.dk

Material and methods

Patients

Seventeen consecutive NSCLC patients with a median age of 63 years (range 44–78 years) were treated with IMRT with curative intent between January and June 2012. One patient was excluded from the present retrospective study because extensive disease necessitated treatment with smaller margins than our institutional standard margins. Supplementary Table I (available online at http://informahealthcare.com/doi/abs/10.3109/0284186X.2013.815798) summarizes key characteristics of the patient group. RT doses of typically 60–66 Gy (Supplementary Table I available online at http://informahealthcare.com/doi/abs/10.3109/0284186X.2013.815798) were delivered in 2 Gy fractions with 5 fractions per week. One patient received only 50 Gy, since higher doses would violate the normal tissue constraints. Fourteen patients were treated for one or more primary tumors and one or more lymph nodes. One patient was treated for a primary tumor target, only, while the operated patient was treated for the tumor bed and lymph nodes.

RT planning and treatment

Figure 1 shows a time line of the treatment course. First, a 3-mm slice thickness, free breathing four-dimensional computed tomography (4DCT) scan was acquired with intravenous contrast application (CT1). An optical breathing signal (RPM, Varian Medical Systems, Palo Alto, CA) was used for phase sorting into 10 phases. The median time interval between planning CT scan and treatment start was 11.5 days (range 7–15 days). The gross tumor volumes of the primary tumor (GTV-t) and the lymph nodes (GTV-n) were delineated in the mid-ventilation phase of the 4DCT scan in a treatment planning system (Eclipse, Varian Medical Systems, CA, USA).

Clinical target volumes (CTV-t and CTV-n) were formed from the GTVs by adding 5 mm isotropic margins and shaping to vessels, bones, and the opposite lung. The CTVs were further expanded to a planning target volume (PTV) by adding margins of 10 mm in the left-right (LR) and anterior-posterior (AP) directions and 13 mm in the cranio-caudal (CC) direction. These margins included contributions from delineation uncertainties, target deformations, respiratory motion, baseline shift, deviations in MLC, couch and CBCT isocenter position, CT distortion and partial volume effects. For the patient receiving post-operative treatment, the CTV-t was contoured directly and subsequently expanded to the PTV. A treatment plan with four to eight 6 MV IMRT beams was created and normalized to give a mean PTV dose equal to 100% of the prescribed dose. Furthermore, the PTV received at least 95% dose while the global maximum was below 107% of the prescribed dose. Dose calculation was done using the AAA algorithm of the treatment planning system [14].

A cone beam CT (CBCT) scan acquired with an On-Board Imager system (Varian Medical Systems) was used for daily image-guided patient setup. The CBCT scan was registered automatically to the planning CT scan based on bony anatomy in a region of interest that included the spine. The registration was evaluated by a radiation therapist and the translational couch correction was calculated and performed automatically.

Dosimetric impact of anatomical changes

A second 4DCT scan (CT2) was acquired halfway through the treatment course in order to investigate possible anatomical changes during the treatment course (Figure 1). CT2 was in mean acquired at fraction number 14 (range fractions 10–16). The mid-ventilation phases of CT1 and CT2 were co-registered
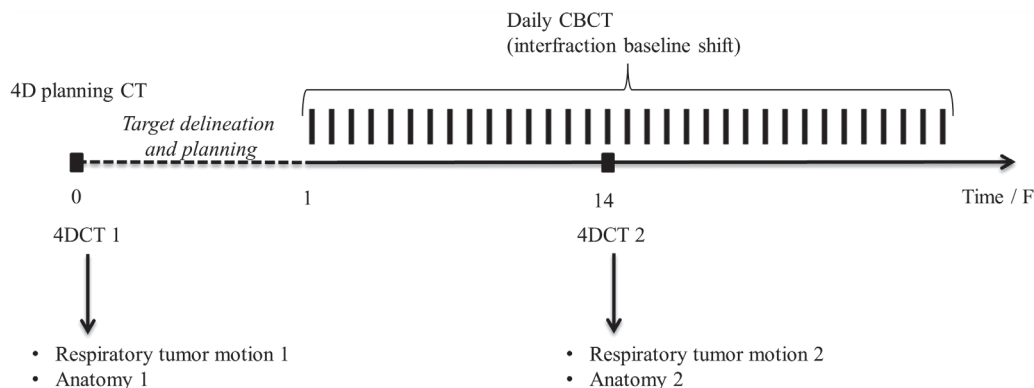

Figure 1. Time line of the entire treatment course including the planning 4DCT scan, daily setup CBCT scans, and the second 4DCT scan acquired approximately at fraction 14.

using both rigid registration of bony anatomy and deformable registration in the Smart Adapt software package (Varian Medical Systems). The rigid registration served two purposes: 1) it was the starting point for the deformable registration; and 2) it was used to transfer the original treatment plan from CT1 to CT2 thus mimicking the bony anatomy-based patient setup procedure. It enabled assessment of the dosimetric effect of the anatomical changes by re-calculation of the treatment plan in the CT2 anatomy. The deformable registration of CT1 and CT2 was performed with a demons algorithm. The driving forces of the algorithm are the intensity differences between the images and gradients in the images. The purpose of the deformable registration was to propagate GTV-t and CTV-t from CT1 to CT2 in order to allow dose evaluation of these target volumes in CT2. To evaluate the volume propagation, the volume of the propagated GTV-t (V_{auto}) was compared with the volume of GTV-t as delineated by a radiation oncologist in the mid-ventilation phase of CT2 (V_{ref}), which was assumed to be the ground truth. Furthermore, the Dice similarity coefficient (DSC) of the two GTV-t volumes was calculated as follows [15]:

$$DSC = \frac{2 \cdot \left(V_{ref} \cap V_{auto} \right)}{V_{ref} + V_{auto}}$$

As a simple measurement of anatomical change the difference between CT1 and CT2 in the water equivalent distance (WED) from the patient surface to the center of GTV-t was measured for each treatment field. The mean WED over all fields was calculated for each patient and compared with the difference in CTV-t mean dose between CT1 and CT2.

Dosimetric impact of internal target motion

Deformable registration was also performed between the mid-ventilation phase and the other phases of CT1 and CT2. The registration was used to propagate GTV-t to all phases of the 4DCT scans. The center-of-mass position of GTV-t in the 10 phases was used as a measure of the respiratory tumor motion at treatment start (CT1) and halfway through the treatment course (CT2). A dose reconstruction method that models target motion as isocenter shifts [16] was used to calculate the CTV-t dose in CT1 and CT2 including the effects of respiratory motion.

In order to measure the daily baseline shifts of the mean tumor position relative to the spine each CBCT scan was rigidly registered to CT1, first based on the spine and then based on the tumor. The difference of the two registrations (spine and tumor) was used as a measure of the interfraction baseline shifts of the tumor. Two patients had a temporary atelectasis showing up in the CBCT scan at three to four fractions during the treatment course. Since the tumor position could not be determined reliably in these CBCT scans the tumor shifts were omitted from the calculations of the baseline shifts.

The daily CBCT tumor baseline shifts were used in motion including reconstructions of the CTV-t dose in CT1 and CT2. Furthermore, the interfraction baseline shift of the tumor relative to the spine in CT2 was determined and compared with the baseline shift in the CBCT scan of the same day. In summary, the CTV-t dose was calculated in both CT1 and CT2 with and without respiratory motion and baseline shifts in order to investigate the dosimetric impact of anatomical changes, respiratory motion and interfraction baseline shifts.

Results

The volumes of GTV-t transferred by deformable image registration from CT1 to CT2 were compared with the GTV-t volumes delineated by the radiation oncologist in CT2. The two GTV-t volumes were highly correlated (R = 0.997, p < 0.001) with a mean (range) difference of 1.2 cm^3 ± 3.9 cm^3 (−7.7–8.1 cm^3) (Supplementary Figure 1, available online at http://informahealthcare.com/doi/abs/10.3109/028 4186X.2013.815798). The mean Dice similarity coefficient was 0.91 (range 0.82–0.95), with the lowest value observed for a small GTV-t of 10 ml. The respiratory tumor motion in the two 4DCT scans was largest in the CC direction and had mean 3D peak-to-peak amplitudes of 4.8 mm ± 3.3 mm (0.9–10.4 mm) and 4.1 mm ± 3.1 mm (0.4–11.0 mm) in CT1 and CT2, respectively. The 3D amplitude in CT1 and CT2 were statistically correlated (R = 0.47, p = 0.002). The interfraction GTV-t baseline shift relative to the spine on average spanned 5.8 mm ± 5.3 mm (2–24 mm) (LR), 7.8 mm ± 4.4 mm (3–18 mm) (CC), and 6.5 mm ± 5.2 mm (3–24 mm) (AP). The absolute mean difference between the interfraction baseline shift in CT2 and the CBCT at the day of acquisition of CT2 was 2 mm (0–4 mm) (LR), 1 mm (0–4 mm) (CC), and 1 mm (0–5 mm) (AP).

Figure 2 shows the mean CTV-t dose for each patient with the anatomy at treatment planning (CT1) and halfway through the treatment course (CT2). The minimum dose delivered to 95% of the CTV-t (D_{95}) showed very similar tendencies as the mean CTV-t doses in Figure 2 (not presented). Transferring the treatment plans from CT1 to CT2 gave rise to an absolute difference in CTV-t mean dose of 1.28% (see Table I). Inclusion of respiratory motion and interfraction baseline shifts induced shifts in the absolute CTV-t mean dose of 0.05 and 0.2% for CT1 and 0.46 and 0.65% for CT2. Comparison of the first and fourth columns in Figure 2
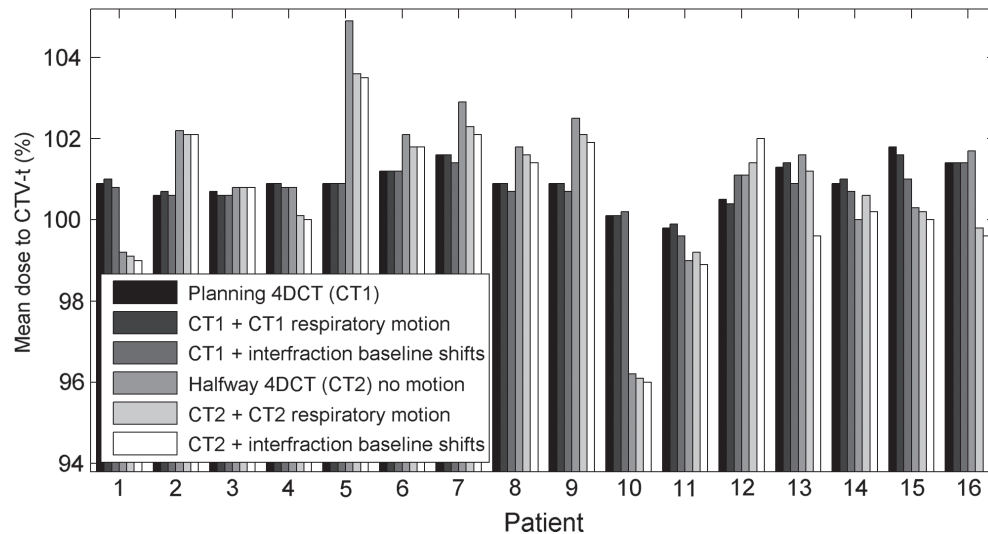
Figure 2. Dosimetric impact of anatomy changes and target motion for all 16 patients. For each patient, the six columns show the mean CTV-t dose for the original static treatment plan in CT1 (column 1), for the same plan with addition of respiratory motion (column 2) and interfraction baseline shifts (column 3), as well as for the treatment plan transferred to CT2 and calculated without motion (column 4) and with respiratory motion (column 5) and interfraction baseline shifts (column 6).

shows that anatomical changes caused changes in the mean CTV-t dose of more than 1% for seven of the 16 patients. For four of these patients, the main anatomical change in CT2 was tumor shrinkage leading to increased mean CTV-t doses (Patients 2, 5, 7 and 9). As an example Figure 3 (top) shows the an increase of 4% in the CTV-t mean dose at CT2 for Patient 5, who had a tumor volume shrinkage of 28% from CT1 to CT2. The other three patients with a substantial change of the mean CTV-t dose, related to anatomical variations had reduced mean CTV-t doses in CT2 caused by a different positioning of the patient's arm (Patient 1), pleural effusion (Patient 10), and a tumor shift due to atelectasis (Patient 15). Figure 3 (bottom) shows the pleural effusion for Patient 10 and the resulting impact on the CTV-t DVH. The change from CT1 to CT2 in mean CTV-t dose correlated with the difference in mean WED to the CTV-t center for the patient group, such that an increased radiological path length to the target center was associated with reduced mean CTV-t dose ($p = 0.022$) (Supplementary Figure 2, available

online at http://informahealthcare.com/doi/abs/10.3109/0284186X.2013.815798). Patients 4, 5, and 16 showed considerable dosimetric effect of respiratory tumor motion in CT2, while Patients 5, 13 and 16 showed a dosimetric change related to the interfraction baseline shifts in CT2. Figure 4 (top) illustrates the dosimetric impact of respiratory motion at CT2 for Patient 16 for whom large CC motion of 10 mm resulted in dose blurring. For Patient 13, interfraction baseline shifts spanning 18 mm resulted in CTV-t underdosage in CT2 as illustrated in Figure 4 (bottom). The dosimetric effects of both respiratory motion and baseline shifts were in general larger in CT2 than in CT1 (Figure 2, Table I), i.e. the treatment plans were more robust against internal tumor motion when calculated in the original CT1 anatomy.

Discussion

We have investigated the dosimetric implication of respiratory tumor motion, interfractional baseline shifts and anatomical changes to the primary target during the course of IMRT for NSCLC patients. It was shown for most patients that the dosimetric impact of anatomical variations was larger than the dosimetric effect of respiratory tumor motion and interfraction baseline shifts for this patient group treated with our standard margins (Table I). Respiratory motion and interfraction baseline shifts showed a larger change in the mean CTV-t dose for the mid-course patient anatomy in CT2 than for the pre-treatment anatomy in CT1. We ascribe this to the fact that the respiratory tumor motion and the

Table I. Absolute differences in CTV-t mean doses between CT1 and CT2 and between CT1 and CT1 including target motion. Similarly for CT2 and CT2 including target motion.

	Mean (%)	Range (%)
Anatomy (CT1, CT2)	1.28	0.1–4.0
Respiratory motion (CT1)	0.05	0–0.2
Interfraction baseline shifts (CT1)	0.20	0–0.8
Respiratory motion (CT2)	0.46	0.1–1.9
Interfraction baseline shifts (CT2)	0.65	0–2.1

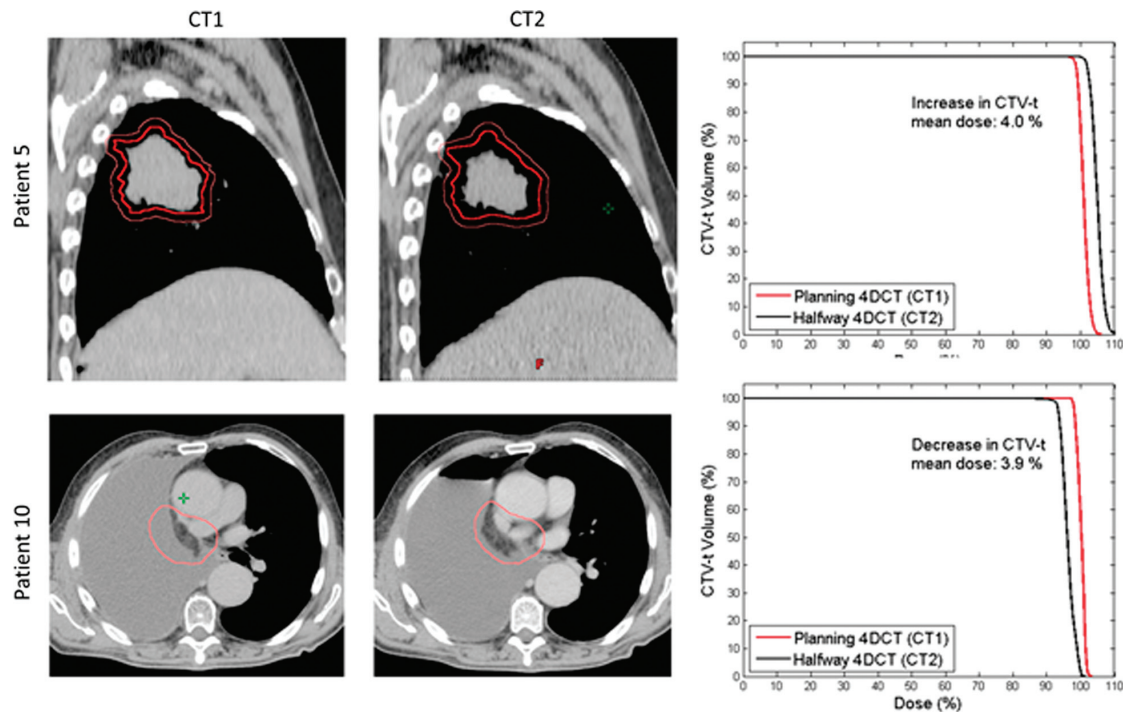CT1, planning 4DCT scan; CT2, mid-course 4DCT scan.

Figure 3. Examples of anatomical changes from the planning 4DCT scan (CT1) to the 4DCT scan (CT2). GTV-t is contoured in red and CTV-t is contoured in pink. Upper panel: Sagittal view of Patient 5 illustrating tumor shrinkage in CT2, and (right) dose volume histograms (DVHs) showing the resulting impact on the CTV-t dose. Lower panel: Transversal CT slices of Patient 10 treated with post-operative RT, illustrating pleural effusion in CT2, and DVHs for CTV-t.

baseline shifts have been taken into account on CT1 through the PTV margins, which make this treatment plan more robust. The anatomy has changed in CT2 and thus, the tumor may no longer be located centrally in the high dose region yielding inferior dose coverage. Furthermore, the homogenous PTV dose in CT1 may be less homogenous when recalculated in the CT2 anatomy, which also leads to
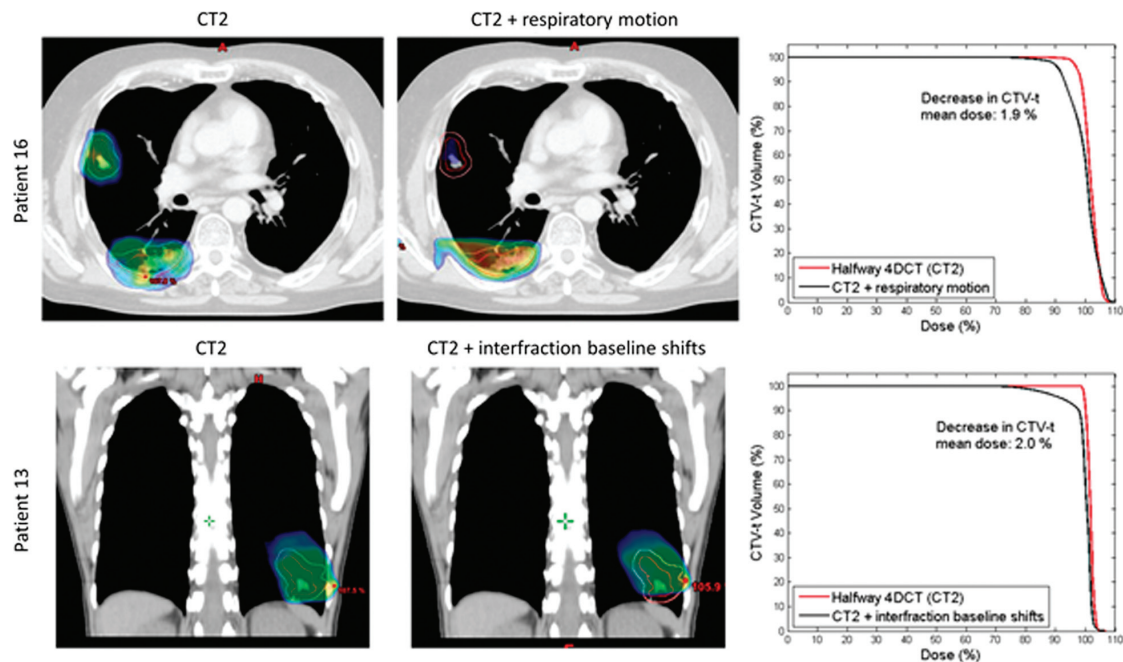

Figure 4. Examples of tumor motion. The GTV-t is contoured in red and CTV-t is contoured in pink. The dose distribution is shown as dose color wash with a minimum dose shown at 95%, and a maximum dose at 107%. Upper: transversal CT slice of Patient 16 at CT2 without and with inclusion of respiratory tumor motion. Lower: Coronal view of Patient 13 at CT2 without and with inclusion of interfraction baseline shifts. The corresponding CTV-t DVHs are shown to the right.

lower robustness against motion. For seven patients there was a difference in the CTV-t mean dose of more than 1% between CT1 and CT2 caused by large anatomical changes such as pleural effusion, atelectasis, and tumor shrinkage. Hugo et al. showed that lung tumor (GTV) regression during RT can introduce geometrical changes in the normal tissue surrounding the tumor that affect the CTV volume, shape and position [8]. Others have reported on changes in lung tumor volume over a treatment course [6,7,13,17].

The current study showed that changes in the WED between CT1 and CT2 correlated with changes in the CTV-t mean dose. The change in WED is used as a measure of the anatomical changes during the treatment since the WED variations are dependent on patient characteristics such as tumor size, tumor position or normal tissue changes. Mori et al. also used the WED measure for the anatomical changes and showed the dosimetric effects of WED changes caused by tumor shrinkage and tissue density changes for charged particle therapy [18].

The large anatomical changes induce large dosimetric changes that cannot be accounted for by increased margins, but instead warrants adaptation of the treatment plan [19]. This is in concordance with the findings of Britton et al., who observed small dosimetric variations on average, but sometimes dramatic dosimetric consequences due to interfractional changes in tumor volume and mobility [11].

Only two of 16 patients had respiratory motion induced changes of the mean CTV-t larger than 1%, indicating a low probability of large dosimetric respiratory motion effects with our current clinical margins. Mechalakos et al. showed that for patients with large breathing amplitudes the respiratory motion plays a significant role in the tumor control probability [20].

From the daily CBCT scans the measured interfraction baseline shifts averaged 5.8–7.8 mm in the three directions. Some patients showed baseline shift up to 24 mm. This is in concordance with other studies [7,17], where the tumor position was found to vary up to 5–10 mm in any direction. Only three patients showed more than 1% change in CTV-t mean dose from interfraction baseline shifts.

The shortcomings of this study include that changes in dose to malignant lymph nodes and surrounding organs were not addressed.

We validated the deformable propagation of GTV-t from CT1 to CT2, by showing a high correlation between the deformable registered volumes and the medical doctor delineation. Additionally, a mean Dice similarity coefficient of 0.91 was obtained, which indicates that the deformable registration worked well in the tumor region. We used the deformable propagation of the CTV-t in the study. The CTV-t propagation is harder to validate by manual delineation since the CTV delineation has larger uncertainties, and the propagation therefore relies on the accuracy of the deformable registration algorithm. The accuracy of the demons algorithm is discussed in several studies [21–23]. Speight et al. found a mean Dice similarity coefficient of 0.86 and a mean distance to agreement of 1 mm for both a B-spline and a demons-based algorithm in a study of 25 lung cancer patients [22]. Nyeng et al. investigated a former version of the demons-based algorithm in Smart Adapt. A comparison of DIR of the inhale and the exhale respiratory phases of 4DCT scans of five patients and DIR of the exhale and the inhale phases (reversed order) showed deviations of 3–6 mm even though ideally, no deviation should be obtained [21]. Brock et al. found absolute mean deviation less than 2 mm in a study of 12 lung cancer patients [23]. This is in concordance with the present study.

Only a quite small dataset per patient was available for assessment of anatomical changes and internal tumor motion. Ideally, the anatomical changes should be recorded by daily 4DCT scans throughout the treatment course rather than by a single mid-course 4DCT scan as in this study. Also, the intrafraction tumor motion should ideally be measured throughout delivery of each treatment fraction, while the respiratory motion was only measured in two 4DCT scans each showing the motion for a single breathing cycle. As a consequence possible intrafraction baseline shifts of the mean tumor position during treatment delivery of each treatment fraction were not included although such shifts may be large for tumors undergoing respiratory motion [24]. Since errors caused by respiratory motion were in effect assumed to be random, causing only blur (and not shifts) of the tumor dose distribution, the dosimetric impact of breathing motion was most probably underestimated in this study. However, the interfraction baseline shifts, measured with daily CBCT scans, included both the random and systematic tumor position shifts throughout the treatment course.

The main finding of this study, that anatomical changes in general resulted in larger dosimetric changes than both respiratory motion and baseline shifts, was specifically made for the current NSCLC patient group with our institutional margins and may not hold for smaller PTV margins, in particular, stereotactic body RT (SBRT) treatments. SBRT patients often have only one target in contrast to NSCLS patients who often have both tumor and lymph node targets, which makes the treatment plan more robust towards respiratory tumor motion.

In conclusion, with the applied margins the anatomical changes had larger impact on the target dose

distribution than respiratory tumor motion and baseline shifts. Large anatomical changes cannot be accounted for by increased margins, so in order to achieve better target coverage throughout the treatment, adaptive RT could be used.

References

[1] Machtay M, Paulus R, Moughan J, Komaki R, Bradley Je, Choy H, et al. Defining local-regional control and its importance in locally advanced non-small cell lung carcinoma. J Thorac Oncol 2012;7:716–22.

[2] Kong F-M, Ten Haken RK, Schipper MJ, Sullivan MA, Chen M, Lopez C, et al. High-dose radiation improved local tumor control and overall survival in patients with inoperable/unresectable non-small-cell lung cancer: Long-term results of a radiation dose escalation study. Int J Radiat Oncol Biol Phys 2005;63:324–33.

[3] van Baardwijk A, Wanders S, Boersma LJ, Borger J, Öllers M, Dingemans AC, et al. Mature results of an individualized radiation dose prescription study based on normal tissue constraints in stages I to III non-small-cell lung cancer. J Clin Oncol 2010;28:1380–6.

[4] Chang JY, Liu HH, Komaki R. Intensity modulated radiation therapy and proton radiotherapy for non-small cell lung cancer. Curr Oncol Rep 2005;7:255–9.

[5] Kupelian PA, Ramsey C, Meeks SL, Willoughby TR, Forbes A, Wagner TH, et al. Serial megavoltage CT imaging during external beam radiotherapy for non-small-cell lung cancer: Observations on tumor regression during treatment. Int J Radiat Oncol Biol Phys 2005;63:1024–8.

[6] Knap MM, Hoffmann L, Nordsmark M, Vestergaard A. Daily cone-beam computed tomography used to determine tumour shrinkage and localisation in lung cancer patients. Acta Oncol 2010;49:1077–84.

[7] Juhler-Nottrup T, Korreman SS, Pedersen AN, Persson G, Aarup LR, Nyström H, et al. Interfractional changes in tumour volume and position during entire radiotherapy courses for lung cancer with respiratory gating and image guidance. Acta Oncol 2008;47:1406–13.

[8] Hugo GD, Weiss E, Badawi A, Orton M. Localization accuracy of the clinical target volume during image-guided radiotherapy of lung cancer. Int J Radiat Oncol Biol Phys 2011; 81:560–7.

[9] Waldeland E, Ramberg C, Arnesen MR, Helland Å, Brustugun OT, Malinen E. Dosimetric impact of a frame-based strategy in stereotactic radiotherapy of lung tumors. Acta Oncol 2012;51:603–9.

[10] Josipovic M, Persson GF, Logadottir Á, Smulders B, Westmann G, Bangsgaard JP. Translational and rotational

[11] Britton KR, Starkschall G, Liu H, Chang JY, Bilton S, Ezhil M, et al. Consequences of anatomic changes and respiratory motion on radiation dose distributions in conformal radiotherapy for locally advanced non-small-cell lung cancer. Int J Radiat Oncol Biol Phys 2009;73:94–102.

[12] Erridge SC, Seppenwoolde Y, Muller SH, van Herk M, De Jaeger K, Belderbos JSA, et al. Portal imaging to assess set-up errors, tumor motion and tumor shrinkage during conformal radiotherapy of non-small cell lung cancer. Radiother Oncol 2003;66:75–85.

[13] Bosmans G, van Baardwijk A, Dekker A, Öllers M, Boersma L, Minken A, et al. Intra-patient variability of tumor volume and tumor motion during conventionally fractionated radiotherapy for locally advanced non-small-cell lung cancer: A prospective clinical study. Int J Radiat Oncol Biol Phys 2006;66:748–53.

[14] Fogliata A, Nicolini G, Vanetti E, Clivio A, Cozzi L. Dosimetric validation of the anisotropic analytical algorithm for photon dose calculation: Fundamental characterization in water. Phys Med Biol 2006;51:1421–38.

[15] Dice LR. Measures of the amount of ecologic association between species. Ecology 1945;26:297–302.

[16] Poulsen PR, Schmidt ML, Keall P, Worm ES, Fledelius W, Hoffmann L. A method of dose reconstruction for moving targets compatible with dynamic treatments. Med Phys 2012;39:6237–46.

[17] Chang J, Mageras GS, Yorke E, De Arruda F, Sillanpaa J, Rosenzweig KE, et al. Observation of interfractional variations in lung tumor position using respiratory gated and ungated megavoltage cone-beam computed tomography. Int J Radiat Oncol Biol Phys 2007;67:1548–58.

[18] Mori S, Lu H-M, Wolfgang JA, Choi NC, Chen GTY. Effects of interfractional anatomic changes on water-equivalent pathlength in charged-particle radiotherapy of lung cancer. J Radiat Res 2009;50:513–9.

[19] Sonke J-J, Belderbos J. Adaptive radiotherapy for lung cancer. Semin Radiat Oncol 2010;20:94–106.

[20] Mechalakos J, Yorke E, Mageras GS, Hertanto A, Jackson A, Obcemea C, et al. Dosimetric effect of respiratory motion in external beam radiotherapy of the lung. Radiother Oncol 2004;71:191–200.

[21] Nyeng TB, Kallehauge JF, Høyer M, Petersen JBB, Poulsen PR, Muren LP. Clinical validation of a 4D-CT based method for lung ventilation measurement in phantoms and patients. Acta Oncol 2011;50:897–907.

[22] Speight R, Sykes J, Lindsay R, Franks K, Thwaites D. The evaluation of a deformable image registration segmentation technique for semi-automating internal target volume (ITV) production from 4DCT images of lung stereotactic body radiotherapy (SBRT) patients. Radiother Oncol 2011;98: 277–83.

[23] Brock KK. Results of a Multi-Institution Deformable Registration Accuracy Study (MIDRAS). Int J Radiat Oncol Biol Phys 2010;76:583–96.

[24] Worm ES, Høyer M, Fledelius W, Poulsen PR. Three-dimensional, time-resolved, intrafraction motion monitoring throughout stereotactic liver radiation therapy on a conventional linear accelerator. Int J Radiat Oncol Biol Phys 2013;86:190–7.

Supplementary material available online

Supplementary Table I and Figures 1, 2.